

## Fast Diazaborine Formation of Semicarbazide Enables Facile Labeling of Bacterial Pathogens

Anupam Bandyopadhyay, Samantha Cambray, and Jianmin Gao

*J. Am. Chem. Soc.*, **Just Accepted Manuscript** • DOI: 10.1021/jacs.6b11115 • Publication Date (Web): 19 Dec 2016

Downloaded from <http://pubs.acs.org> on December 20, 2016

### Just Accepted

“Just Accepted” manuscripts have been peer-reviewed and accepted for publication. They are posted online prior to technical editing, formatting for publication and author proofing. The American Chemical Society provides “Just Accepted” as a free service to the research community to expedite the dissemination of scientific material as soon as possible after acceptance. “Just Accepted” manuscripts appear in full in PDF format accompanied by an HTML abstract. “Just Accepted” manuscripts have been fully peer reviewed, but should not be considered the official version of record. They are accessible to all readers and citable by the Digital Object Identifier (DOI®). “Just Accepted” is an optional service offered to authors. Therefore, the “Just Accepted” Web site may not include all articles that will be published in the journal. After a manuscript is technically edited and formatted, it will be removed from the “Just Accepted” Web site and published as an ASAP article. Note that technical editing may introduce minor changes to the manuscript text and/or graphics which could affect content, and all legal disclaimers and ethical guidelines that apply to the journal pertain. ACS cannot be held responsible for errors or consequences arising from the use of information contained in these “Just Accepted” manuscripts.



# Fast Diazaborine Formation of Semicarbazide Enables Facile Labeling of Bacterial Pathogens

Anupam Bandyopadhyay,<sup>§</sup> Samantha Cambray,<sup>§</sup> and Jianmin Gao\*

<sup>§</sup>These authors contributed equally to this work

\*Correspondence should be directed to jianmin.gao@bc.edu

## Abstract

Bioorthogonal conjugation chemistry has enabled the development of tools for the interrogation of complex biological systems. Although a number of bioorthogonal reactions have been documented in literature, they are less ideal for one or several reasons including slow kinetics, low stability of the conjugated product, requirement of toxic catalysts, and side reactions with unintended biomolecules. Herein we report a fast ( $>10^3 \text{ M}^{-1}\text{s}^{-1}$ ) and bioorthogonal conjugation reaction that joins semicarbazide to an aryl ketone or aldehyde with an *ortho*-boronic acid substituent. The boronic acid moiety greatly accelerates the initial formation of a semicarbazone conjugate, which rearranges into a stable diazaborine. The diazaborine formation can be performed in blood serum or cell lysates with minimal interference from biomolecules. We further demonstrate that application of this conjugation chemistry enables facile labeling of bacteria. A synthetic amino acid D-AB3, which presents a 2-acetylphenylboronic acid moiety as its side chain, was found to incorporate into several bacterial species through cell wall remodeling, with particularly high efficiency for *Escherichia coli*. Subsequent D-AB3 conjugation to a fluorophore-labeled semicarbazide allows robust detection of this bacterial pathogen in blood serum.

## Introduction

Bioorthogonal reactions have emerged as powerful and enabling technologies in biomedical research and technology development.<sup>1-6</sup> For applications in live cells and organisms, an ideal bioorthogonal reaction is expected to exhibit fast reaction kinetics, high orthogonality to endogenous reactive groups, low toxicity and high stability of the reagents, as well as the products. Despite the large body of literature reports, few reactions meet all the criteria described above.<sup>7</sup> Much interest remains in fast conjugation reactions that are truly compatible with biological systems.

Among the earliest known bioorthogonal reactions, oxime and hydrazone formation of  $\alpha$ -nucleophiles has only found limited applications in live cells and organisms. This is largely due to the slow kinetics of such reactions under physiologic conditions, as well as the sub-optimal stability of the conjugation products. For example, a typical hydrazone exhibits a half-life of only a couple of hours in neutral aqueous media.<sup>8</sup> In terms of reaction kinetics, the conjugation between phenylhydrazine and benzaldehyde is barely detectable at neutral pH. Even with acid and aniline catalysis,<sup>9,10</sup> this conjugation reaction gives rate constants around  $1 \text{ M}^{-1} \text{ s}^{-1}$ , indicating that the reaction requires 3 hours to be half complete even with reactants at  $100 \text{ }\mu\text{M}$  concentrations. In contrast to the sluggish hydrazone formation, Dewar and Snyder in the early 1960s documented that, when mixed in water, phenylhydrazine conjugated instantaneously with 2-formylphenyl boronic acid (2-FPBA) to give a diazaborine heterocycle in quantitative yield.<sup>11</sup> Interestingly, the diazaborine product was found to survive boiling in solutions of either 10% HCl or 10% KOH. Recent and more detailed studies by the Bane<sup>12</sup> and Gillingham<sup>13</sup> groups revealed that the 2-FPBA-phenylhydrazine conjugation proceeds with rate constants over  $10^3 \text{ M}^{-1} \text{ s}^{-1}$ . Despite the fast kinetics, this conjugation reaction remains less ideal for biological applications due to the poor stability and cytotoxicity of phenylhydrazine (*vide infra*), in addition to the high reactivity of 2-FPBA toward endogenous cysteines.<sup>14</sup> Herein we report the fast diazaborine formation of semicarbazide, which shows much improved stability in biological milieu. Importantly, we demonstrate that semicarbazide readily conjugates with not only 2-FPBA, but also the ketone analogue 2-acetylphenylboronic acid (2-APBA), which avoids the interference of endogenous cysteines.

## Results

### Semicarbazide conjugates with 2-FPBA and 2-APBA to form diazaborines

The rapid conjugation of phenylhydrazine to form diazaborines is attractive as a bioorthogonal reaction. However, phenylhydrazine is prone to oxidation resulting in a short half-life of only several hours in neutral aqueous media (Figure S1, SI). Lending further evidence to its degradation, an aged sample of phenylhydrazine failed to form diazaborine with 2-APBA (Figure S1, SI). In addition to the poor stability, the high reactivity of phenylhydrazine often leads to cytotoxicity (*vide infra*), which makes it impractical for biological applications. The more stable  $\alpha$ -nucleophiles, such as acetylhydrazide and benzhydrazide, were found to reversibly conjugate with 2-APBA to form iminoboronates instead of diazaborines.<sup>15</sup> In search for stable surrogates of phenylhydrazine toward diazaborine formation, we found that semicarbazide remains stable in neutral buffer for weeks (Figure S1, SI), and importantly, it readily conjugates with 2-FPBA and 2-APBA to give diazaborines. Mixing semicarbazide with 2-FPBA in a neutral buffer resulted in a clean NMR spectrum corresponding to a single conjugation product (DAB1, Figure 1a, b). We were able to crystallize DAB1 (Figure 1c), which clearly revealed an amide-substituted diazaborine heterocycle. Excitingly, mixing semicarbazide with 2-APBA, the ketone analogue of 2-FPBA, also resulted in quick conjugation, with DAB2 formation observed as soon as the NMR spectrum could be taken (< 5min) (Figure 1a). The NMR and mass-spec data of the conjugation product are consistent with diazaborine formation as well (Figure 1b, Figure S2, SI). Our initial attempts to crystallize DAB2 were unsuccessful due to its poor solubility in water and several organic solvents. The poor solubility likely originates from the planar structure of the postulated DAB2 structure, which favors stacking instead of dissolving into solution. To overcome the solubility problem, we thought to use a recently reported amino acid L-AB3 that incorporates the 2-APBA moiety as its side chain.<sup>16</sup> Semicarbazide was found to readily conjugate with a protected form of AB3 (Boc-L-AB3(pin)-O<sup>t</sup>Bu) and the product crystallized out of a water/methanol mixture. The X-ray structure confirmed the diazaborine formation of the AB3 side chain (DAB3, Figure 1d). The diazaborine heterocycle of DAB3 is essentially superimposable with the crystal structure of DAB1. To the best of our knowledge, this is the first crystal structure of diazaborine synthesized from a ketone, although there are documented structures for diazaborines derived from aldehydes.<sup>17</sup>

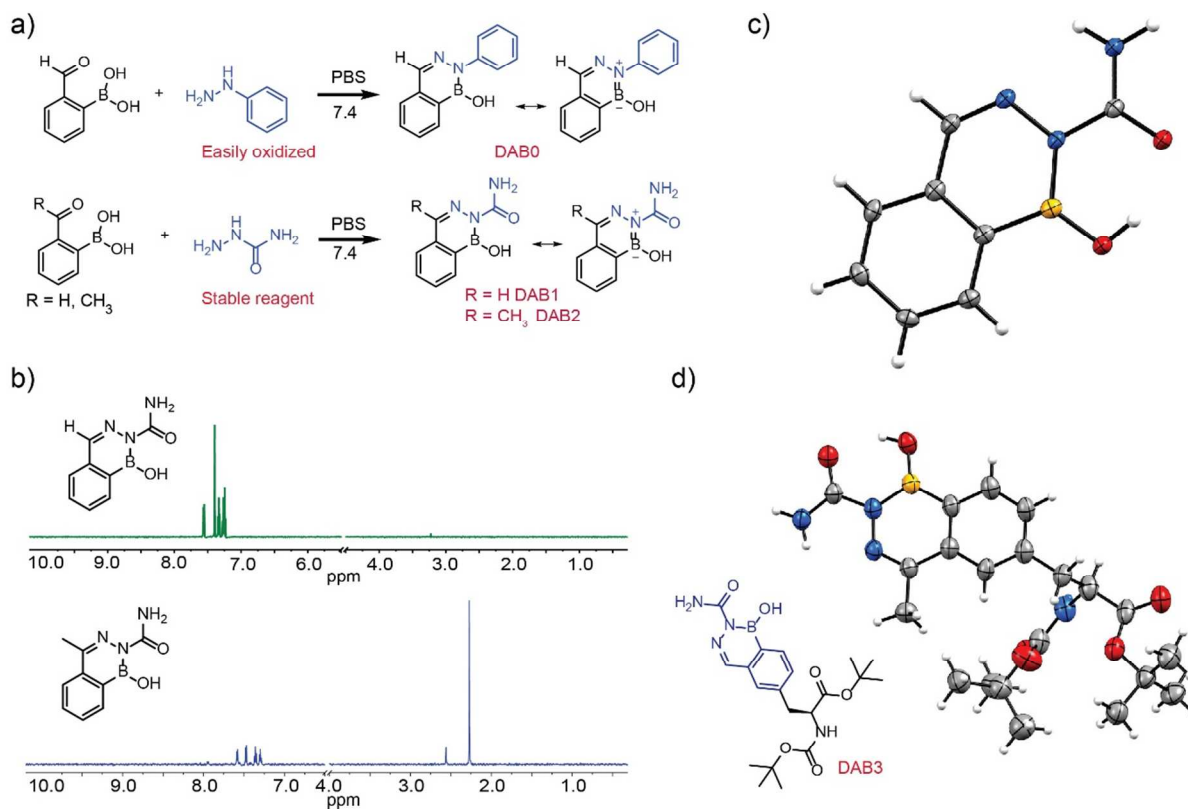


**Figure 1. Diazaborine formation of semicarbazide.** a) Schematic illustration of diazaborine formation of semicarbazide in comparison to that of phenylhydrazine. b) <sup>1</sup>H-NMR spectra of semicarbazide mixed with equimolar 2-FPBA (top) and 2-APBA (bottom) respectively. c) Crystal structure of DAB1, the diazaborine conjugate of semicarbazide with 2-FPBA. d) Crystal structure of DAB3, a diazaborine conjugate of semicarbazide with the synthetic amino acid L-AB3.

#### Diazaborine formation of semicarbazide is fast and irreversible

Similar to phenylhydrazine, semicarbazide conjugation with 2-FPBA or 2-APBA gives stable diazaborine products in aqueous solution. First, DAB1 and DAB2 both remained intact during LC analysis and purification, which were performed with acidic eluents (Figure S3, SI). In contrast, the 2-APBA conjugate of acetylhydrazide or benzhydrazide could not be identified in LC-MS analysis due to complete hydrolysis.<sup>15</sup> Furthermore, NMR samples of DAB1 and DAB2 prepared in a neutral buffer (100 μM) showed no degradation over three days at room temperature (Figure 2a, Figure S4, SI). To define whether the observed stability has a thermodynamic or kinetic origin, we prepared control samples by mixing semicarbazide (100 μM) with equimolar 2-FPBA and 2-APBA respectively. As revealed by <sup>1</sup>H-NMR

analysis, 2-FPBA completely conjugated with semicarbazide under these conditions, while the mixture of 2-APBA and semicarbazide reached a maximum yield of 80% with 20% reactants remaining (Figure 1b, Figure 2a). The incomplete conjugation of 2-APBA contrasts the lack of degradation of DAB2, indicating that the diazaborines of semicarbazide are kinetically stable, which is highly desirable for bioconjugation reactions.

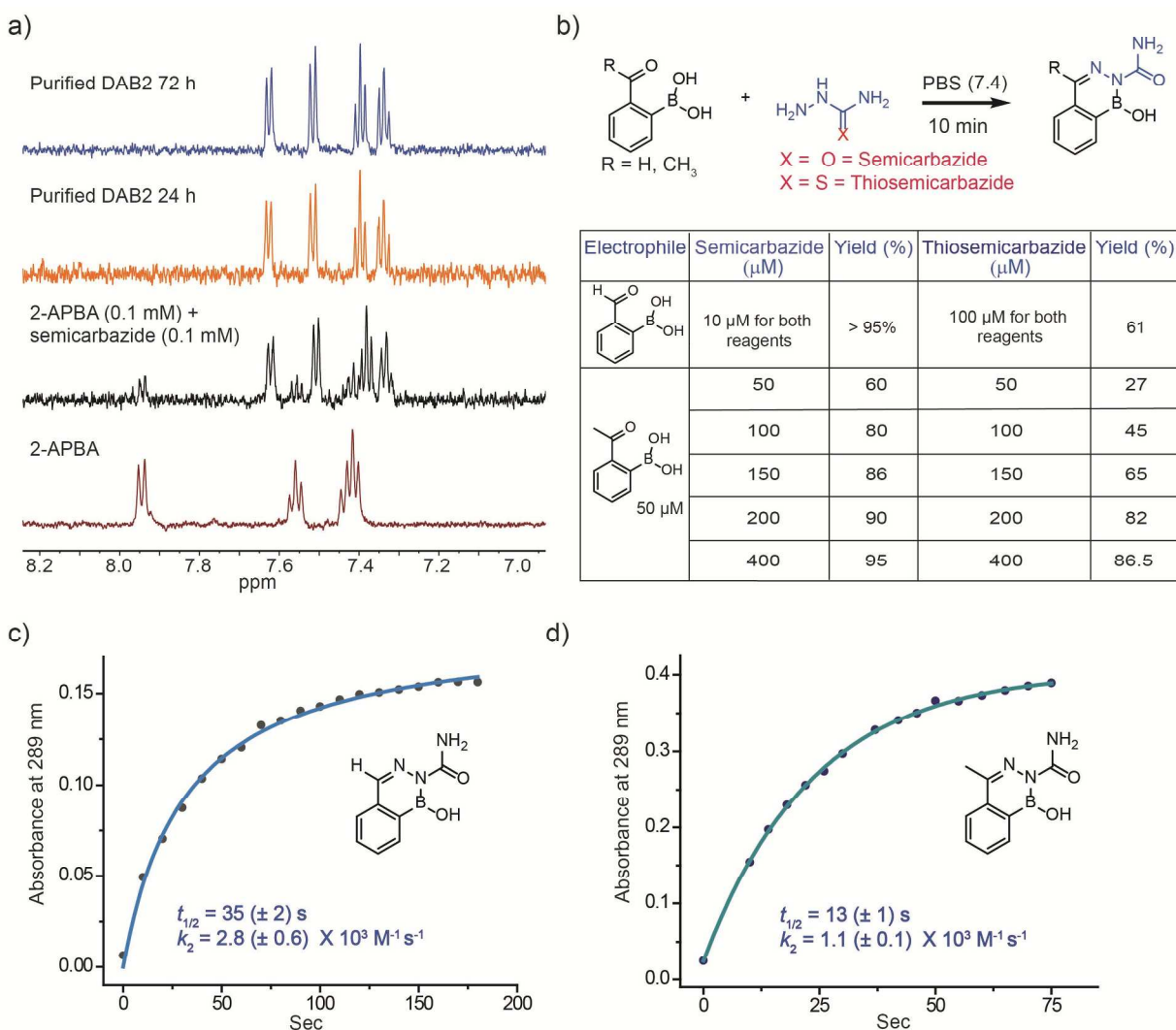


**Figure 2. Stability, efficiency and kinetics of formation of diazaborines.** a)  $^1\text{H}$ -NMR analysis of DAB2 formation as well as potential decomposition demonstrating the kinetic stability of DAB2. b) Yields of diazaborine formation for various combinations of reactants as determined by  $^1\text{H}$  NMR. Due to the fast kinetics, all reactions went to completion within 10 min. c) A representative kinetic profile of DAB1 formation monitored by UV-vis spectroscopy. d) A representative kinetic profile of DAB2 formation monitored by UV-vis spectroscopy. The kinetic measurements were performed three times and the

1  
2  
3 error values for  $t_{1/2}$  and  $k_2$  were reported as the standard deviations of the three trials. Details of curve  
4 fitting are provided in SI.  
5  
6  
7

8  
9 The conjugation efficiency of semicarbazide was examined by  $^1\text{H-NMR}$  and LC-MS (Figure 2b, Figure S5-  
10 6, SI). The results show that DAB1 formation proceeded quantitatively even with the reactants at low  
11 micromolar concentrations (Figure S5, SI). In comparison, DAB2 formation was found to be somewhat  
12 less efficient: with 2-APBA at 50  $\mu\text{M}$ , equimolar semicarbazide afforded 60% yield of DAB2 and ~95%  
13 yield was obtained with semicarbazide at 400  $\mu\text{M}$  (Figure 2b, Figure S6a, SI). The LC-MS analysis gave  
14 consistent results with the slightly lower percentages of the product peak (Figure S6b, SI), possibly due  
15 to the variations of absorptivity with the starting material and product in HPLC solvents. It is somewhat  
16 surprising that DAB2 formation does not go to completion given that the reaction is irreversible and  
17 there is no side product. To understand this phenomenon, we have probed the possibility of product  
18 inhibition by recording the  $^1\text{H NMR}$  spectra of a DAB2 derivative mixed with each reactant at equimolar  
19 concentrations (1 mM). Due to the low water solubility of DAB2, the diazaborine conjugate of  
20 semicarbazide and the amino acid L-AB3 was used for this experiment. The NMR spectra revealed a  
21 noticeable shift of the aromatic peaks of the diazaborine conjugate when mixed with either reactant  
22 (Figure S7). The peak shift presumably originates from interactions of the product with the reactants,  
23 which may be responsible for the stalled reactions. Similar to semicarbazide, we found that  
24 thiosemicarbazide also rapidly conjugated with 2-FPBA and 2-APBA to give diazaborines. However,  
25 thiosemicarbazide gave lower yields in comparison to semicarbazide (Figure 2b, Figure S8, SI). For  
26 example, at 100  $\mu\text{M}$  concentrations, thiosemicarbazide conjugates with 2-FPBA to give ~60% yield, while  
27 no diazaborine formation was observed at 10  $\mu\text{M}$  concentrations.  
28  
29  
30  
31  
32  
33  
34  
35  
36  
37  
38  
39  
40  
41

42 The kinetics of diazaborine formation was determined via a UV-vis experiment, which allowed the  
43 reaction to be monitored at low concentrations (Figure S9, SI). Both 2-FPBA and 2-APBA exhibit an  
44 absorption maximum at 254 nm, which shifts to ~ 290 nm upon diazaborine formation. The kinetics of  
45 DAB1 formation was assessed by mixing 2-FPBA and semicarbazide at 10  $\mu\text{M}$  concentrations. Monitoring  
46 the absorption increase at 290 nm over time afforded a kinetic plot of the reaction (Figure 2c), fitting of  
47 which according to a second order reaction mechanism (see SI for details) gave a rate constant of  $>10^3$   
48  $\text{M}^{-1} \text{s}^{-1}$ . A similar rate constant was obtained for the conjugation between semicarbazide and 2-APBA  
49 (Figure 2d). These results show that the diazaborine formation of semicarbazide is equally fast as that of  
50 phenylhydrazine<sup>12,13</sup> and comparable to the fastest conjugation reactions documented in literature.<sup>18-21</sup>  
51  
52  
53  
54  
55  
56  
57  
58  
59  
60

1  
2  
3 Bioorthogonality of the diazaborine formation of semicarbazide  
4

5  
6 A recent report from our group<sup>14</sup> describes that the 2-FPBA-cysteine conjugation proceeds to  
7 completion even at low micromolar concentrations, which is well below the concentrations of cysteine  
8 in a cell.<sup>22</sup> Although reversible, the dissociation of the 2-FPBA-cysteine adduct only occurs over the  
9 course of hours. The cysteine reactivity of 2-FPBA might interfere with its conjugation with  
10 semicarbazide. Indeed, 2-FPBA pre-incubated with equimolar free cysteine (0.2 mM) only gave 40%  
11 diazaborine after reaction with semicarbazide for 40 min (Figure 3a). For comparison, the reaction  
12 should complete to 100% within less than 3 min in a cysteine free medium (Figure 2c). Interestingly, 2-  
13 APBA was found to only conjugate with cysteine at millimolar concentrations (Figure 3b). Furthermore,  
14 the 2-APBA-cysteine conjugation is rapidly reversible as shown by a dilution experiment, in which the  
15 proton resonances of the conjugate decreased instantaneously after a 10 x dilution (Figure 3b).  
16 Consistent with these observations, pre-incubation of 2-APBA with cysteine (0.2 mM) resulted in no  
17 difference in DAB2 formation (Figure 3a), suggesting a wide applicability of the 2-APBA-semicarbazide  
18 conjugation reaction.  
19  
20  
21  
22  
23  
24  
25  
26  
27  
28  
29  
30  
31  
32  
33  
34  
35  
36  
37  
38  
39  
40  
41  
42  
43  
44  
45  
46  
47  
48  
49  
50  
51  
52  
53  
54  
55  
56  
57  
58  
59  
60

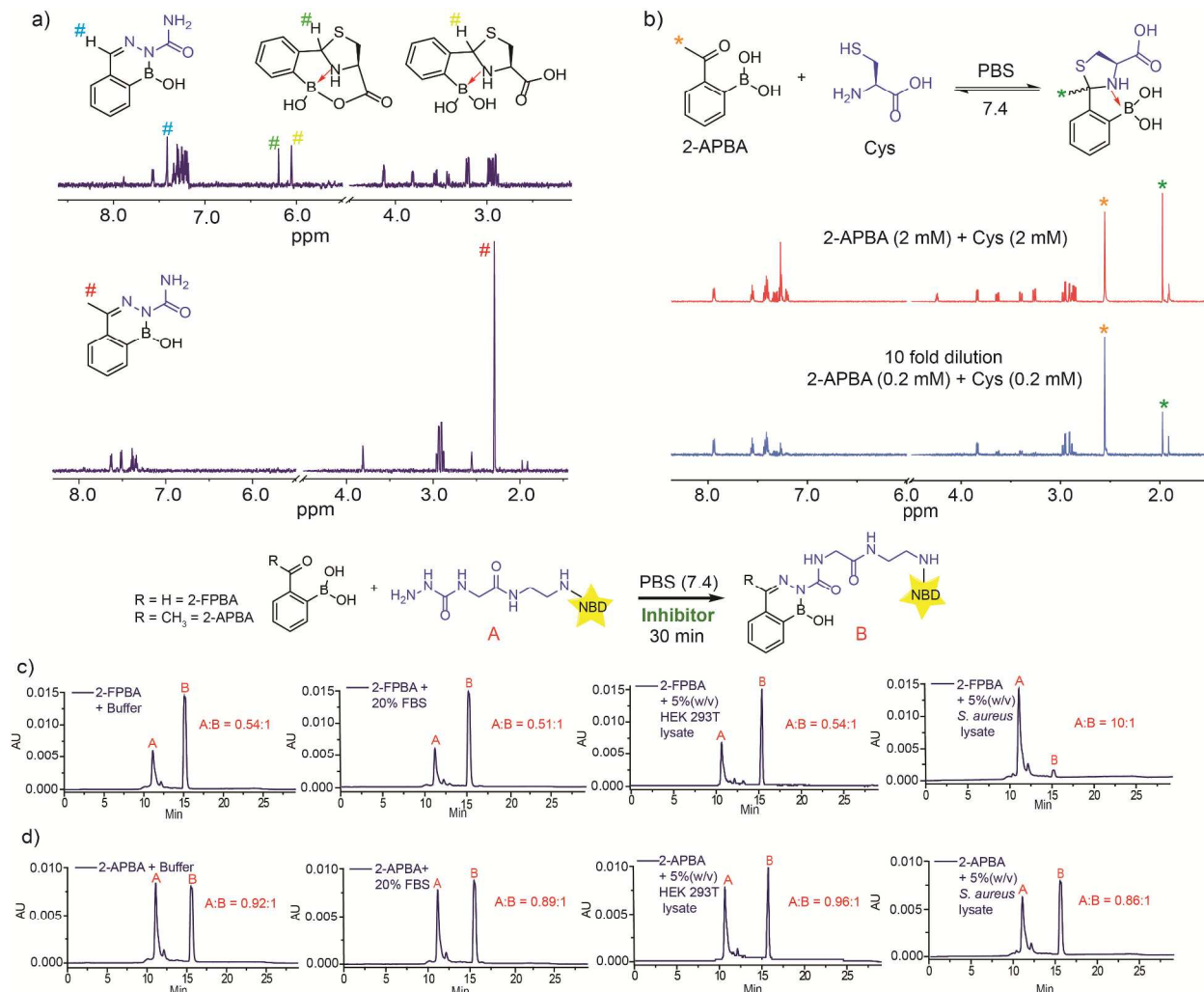


**Figure 3. Compatibility and orthogonality of the diazaborine chemistry to biological systems.** a)  $^1\text{H-NMR}$  spectra illustrating the weak affinity and rapid reversibility of the 2-APBA-cysteine conjugation. b)  $^1\text{H-NMR}$  analysis showing that the diazaborine formation of 2-FPBA, but not 2-APBA, is inhibited by the presence of free cysteine. All reactants were used at 0.2 mM in a pH 7.4 buffer. The reaction mixtures were incubated for 40 min before analysis. c) DAB1 and d) DAB2 formation in buffer alone and in presence of FBS (20%, v/v), HEK cell lysate (5 mg/mL), *S. aureus* cell lysate (5 mg/mL) respectively. For c) and d), the samples were prepared with 25  $\mu\text{M}$  2-FPBA or 2-APBA and 50  $\mu\text{M}$  Scz-NBD in a pH 7.4 buffer. The LC traces were recorded after 30 min incubation. The relative peak areas of Scz-NBD over the diazaborine product are shown on the LC traces and used to estimate the conversion of the reactions.

The diazaborine formation of semicarbazide was further assessed for bioorthogonality with the addition of fetal bovine serum (FBS), as well as lysates of bacterial and mammalian cells. The presence of 20%

1  
2  
3 FBS in the reaction media resulted in little interference to the diazaborine formation of both 2-FPBA and  
4 2-APBA (Figure 3c, d). This is perhaps not surprising considering the oxidative environment of blood  
5 serum, which results in low concentrations of free cysteine.<sup>23</sup> Interestingly, the diazaborine formation of  
6 both 2-FPBA and 2-APBA was minimally affected by the presence of a mammalian cell lysate (HEK 293T  
7 cells, 5 mg/mL). This lack of inhibition can be rationalized by the drop of free cysteine concentration in  
8 the cell lysate due to dilution and possible oxidation during lysate preparation. In contrast, the presence  
9 of *S. aureus* cell lysate (5 mg/mL) did inhibit the conjugation of 2-FPBA to semicarbazide, giving only 12%  
10 product over 30 min (Figure 3c). Aside from free cysteine, *S. aureus* is known to express high  
11 concentrations of bacillithiol,<sup>24</sup> which displays an N-terminal cysteine and is likely responsible for the  
12 observed inhibition of the diazaborine formation of 2-FPBA. With the presence of *S. aureus* cell lysate,  
13 the diazaborine product of 2-FPBA was found to increase over a time course of several hours (Figure  
14 S10, SI). The slow progression of the reaction is consistent with the dissociation kinetics of the 2-FPBA-  
15 cysteine conjugate. Excitingly, in contrast to 2-FPBA, 2-APBA rapidly conjugated with semicarbazide with  
16 no interference by the *S. aureus* cell lysate (Figure 3d). This further showcases the bioorthogonality of  
17 the 2-APBA and semicarbazide conjugation reaction.  
18  
19  
20  
21  
22  
23  
24  
25  
26  
27  
28  
29

#### 30 Assessing the stability and toxicity of the reagents used for diazaborine conjugation

31  
32 To test the stability of the reagents in biological media, we have respectively incubated 2-FPBA, 2-APBA  
33 and a FITC-labeled semicarbazide (Scz-FITC) with either 20% FBS or the HEK cell lysate for 24 hr before  
34 subjecting them to the diazaborine conjugation reactions. HPLC analysis of the reactions showed  
35 essentially the same yields regardless of the long incubation with FBS or the cell lysate (Figure S11, SI).  
36 The stability of the semicarbazide is quite remarkable in comparison to the quick degradation of  
37 phenylhydrazine (Figure S1, SI). Consistent with these observations, gel analysis of the HEK cell lysate  
38 treated with Scz-FITC revealed no significant protein labeling by Scz-FITC (Figure S12, SI). Collectively,  
39 these results confirm the stability of all three reagents and showcase the robustness of these  
40 diazaborine conjugation reactions.  
41  
42  
43  
44  
45  
46  
47  
48

49 We further examined the potential cytotoxicity of semicarbazide together with phenylhydrazine for  
50 comparison (Figure 4). Two strains of bacteria (*E. coli* and *S. aureus*) and a model mammalian cell line  
51 (HEK 293T) were treated with semicarbazide and phenylhydrazine respectively. The percentages of cell  
52 survival were determined through colony counting for the bacteria and the MTT assay for the HEK cells.  
53 The results revealed little toxicity of semicarbazide for all three cell lines tested. In comparison,  
54 phenylhydrazine elicited 10-25% cell death for the bacteria and ~50% cell death for the HEK cells after  
55  
56  
57  
58  
59  
60

24 hrs of incubation. We also tested the toxicity of a 2-APBA derivative (D-AB3, structure shown in Figure 5), which under the same conditions elicited no measurable death for any of the cell lines. These observations collectively showcase the robustness and remarkable compatibility of the diazaborine chemistry to biological systems.

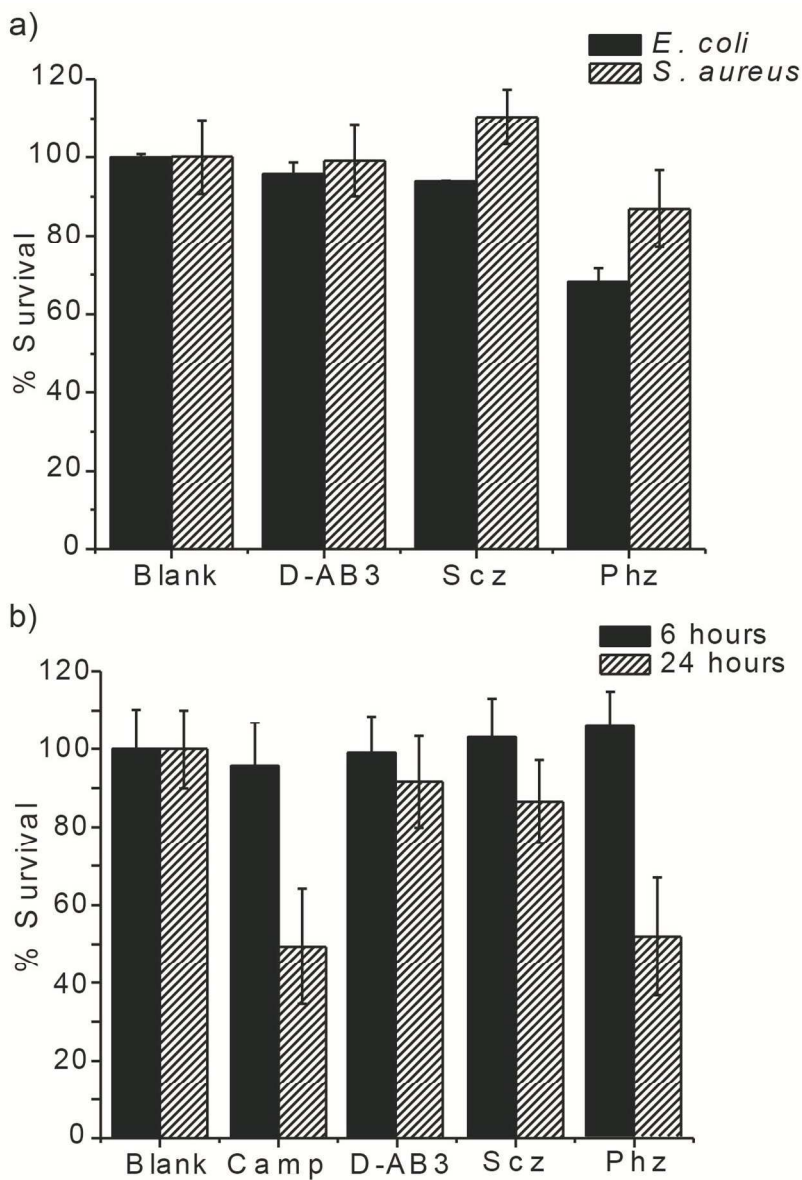
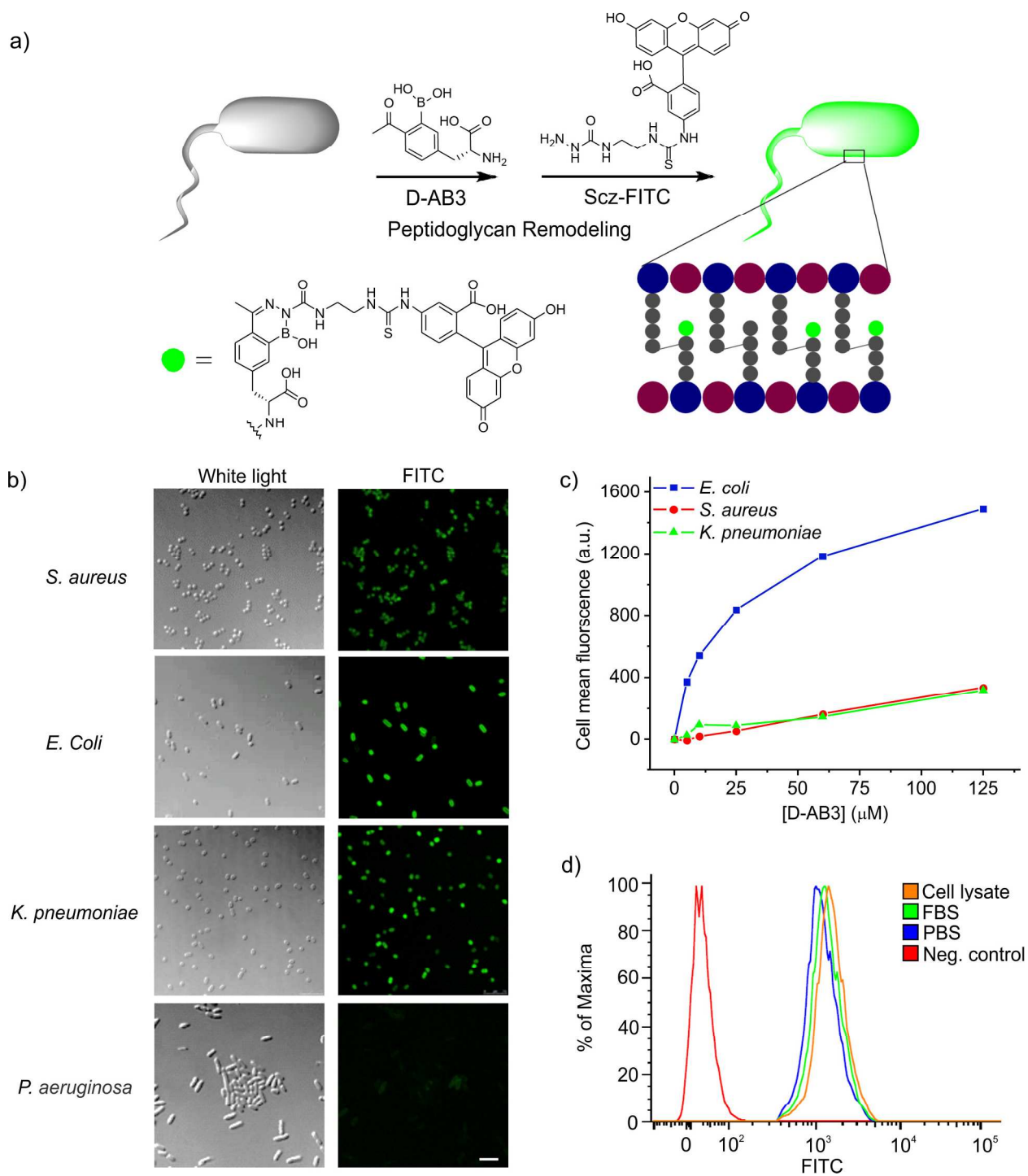


**Figure 4. Cytotoxicity studies of the reactants for diazaborine conjugation.** a) Percentage of cell survival determined by colony counting for *E. coli* and *S. aureus*. b) Percentage of cell survival determined by the MTT assay for HEK 293T cells. Phenylhydrazine (Phz) was included as a direct comparison to

semicarbazide (Scz). Camptothecin (Camp) was used as a positive control in the MTT assay of HEK 293T cells. All compounds were tested at 50  $\mu\text{M}$  concentration.



1  
2  
3 **Figure 5. Semicarbazide ligation enables bacterial labeling.** a) Schematic illustration of the two-step (D-  
4 AB3 followed by Scz-FITC) protocol for bacterial cell labeling. b) Microscopic images showing that the D-  
5 AB3 and Scz-FITC treatment gives varied degrees of labeling across bacterial species. c) Flow cytometry  
6 results corroborating the *E. coli* selectivity of the D-AB3 and Scz-FITC staining protocol. The  
7 concentration dependence data were analyzed according to Michaelis-Menten kinetics (Figure S21) and  
8 discussed in the text. d) Flow cytometry histograms showing the semicarbazide-enabled bacterial  
9 labeling is unaffected by blood serum or cell lysate. All labeling experiments were performed with 50  
10  $\mu\text{M}$  Scz-FITC.  
11  
12  
13

### 14 15 16 Semicarbazide conjugation allows facile labeling of bacterial pathogens 17

18  
19 As an exemplary application in biological systems, we assessed the potential of the diazaborine  
20 chemistry of semicarbazide for labeling bacterial pathogens. Facile detection and quick identification of  
21 pathogenic bacteria are highly desirable in clinic as well as in environmental settings.<sup>25</sup> Recently a series  
22 of publications show that bacterial peptidoglycan undergoes dynamic remodeling, through which  
23 synthetic amino acids and even selected dipeptides can be incorporated into the cell wall network.<sup>26-34</sup>  
24 We postulated that incorporating a 2-FPBA or 2-APBA moiety into the bacterial cell wall followed by  
25 semicarbazide ligation should allow facile labeling of bacterial cells. To test this hypothesis, we have  
26 synthesized the amino acid AB3 in the D-configuration (D-AB3, Figure 5a). D-AB3 was chosen over the  
27 aldehyde analogue to avoid any complications of cysteines and cysteine derivatives. Several strains of  
28 pathogenic bacteria, including *Staphylococcus aureus* (*S. aureus*), *Escherichia coli* (*E. coli*), *Klebsiella*  
29 *pneumoniae* (*K. pneumoniae*), and *Pseudomonas aeruginosa* (*P. aeruginosa*), were treated with D-AB3 at  
30 varied concentrations for varied time span. After washing away the excess D-AB3, the cells were stained  
31 with Scz-FITC (Figure 5a, Figure S13-16, SI). The semicarbazide ligation was performed with 50  $\mu\text{M}$  Scz-  
32 FITC over 30 min; under these conditions the conjugation is expected to be >60% complete (Figure S6  
33 and S17, SI). After stringent washing, the cells were analyzed by fluorescence microscopy and flow  
34 cytometry. Interestingly, the bacterial strains showed varied degrees of labeling under a fluorescence  
35 microscope (Figure 5b). While the treated *E. coli* cells showed bright fluorescence, *P. aeruginosa* was not  
36 stained at all. *S. aureus* and *K. pneumoniae* were also stained, albeit with significantly lower efficiency in  
37 comparison to *E. coli*. The preferential labeling of *E. coli* by D-AB3 was further validated by a co-culture  
38 experiment, for which the D-AB3 treated *E. coli* and *S. aureus* cells were mixed and then labeled with  
39 Scz-FITC. The microscopic images of the co-culture clearly demonstrated the selective labeling of *E. coli*,  
40 which displayed strong fluorescence while the *S. aureus* cells appeared dim (Figure 18, SI). The more  
41 efficient incorporation of D-AB3 into *E. coli* was further validated by flow cytometry analysis, which gives  
42  
43  
44  
45  
46  
47  
48  
49  
50  
51  
52  
53  
54  
55  
56  
57  
58  
59  
60

1  
2  
3 mean cell fluorescence intensity near ten times higher than that of *S. aureus* and *K. pneumoniae* (Figure  
4 5c). As expected for the high orthogonality of the diazaborine chemistry to biological systems, the  
5 6 bacterial cell staining showed little inference by the presence of blood serum or a cell lysate (Figure 5d).  
7 8 Specifically we treated the *E. coli* cells with D-AB3 and then labeled with Scz-FITC in the presence of 5  
9 10 mg/mL HEK 293T cell lysate and 10% (v/v) FBS, respectively. Flow cytometry analysis of these samples  
11 12 yielded comparable histograms of the stained cells, again demonstrating the remarkable compatibility of  
13 14 the diazaborine chemistry with biological systems.

15  
16 Importantly, treating cells with L-AB3 through the same protocol yielded minimal fluorescence staining  
17 18 regardless of the bacterial strains used (Figure S19, SI). This provides strong support for the  
19 20 peptidoglycan remodeling mechanism, in which D-AB3 is incorporated into the cell wall, while L-AB3  
21 22 cannot be accepted by the transpeptidases responsible for peptidoglycan remodeling.<sup>27</sup> Further, the  
23 24 confocal microscopy images showed the cell envelope location of fluorescence (Figure S20, SI), lending  
25 26 further support to the peptidoglycan remodeling mechanism for D-AB3 incorporation. Given the high  
27 28 specificity of Scz-FITC for D-AB3, the fluorescence of the labeled cells should reflect on the amount of D-  
29 30 AB3 incorporated into peptidoglycans. More quantitative analysis of D-AB3 uptake by *E. coli* was done by  
31 32 plotting the cell mean fluorescence against D-AB3 concentration (Figure 5c, Figure S21, SI). The plot  
33 34 displays a saturating profile as expected for an enzyme catalyzed reaction. This is consistent with the  
35 36 previous report that D-amino acid incorporation is mediated by the transpeptidases.<sup>27</sup> Fitting the data  
37 38 according to the Michaelis-Menten mechanism yields a  $K_M$  value of 23  $\mu\text{M}$  (Figure S21, SI). This  $K_M$  value  
39 40 is about an order of magnitude lower than that of a D-Lys derivative used for *S. aureus* labeling,<sup>32</sup>  
41 42 suggesting the D-AB3 uptake by *E. coli* is highly efficient. The concentration profile of D-AB3 for *S. aureus*  
43 44 staining data displays a linear relationship, suggesting the  $K_M$  value is well above the highest  
45 46 concentration tested (125  $\mu\text{M}$ , Figure S21, SI). Although a precise  $K_M$  value cannot be obtained for *S.*  
47 48 *aureus*, the slope of the linear fit should be proportional to the catalytic efficiency of the relevant  
49 50 enzyme ( $V_{max}/K_M$ ). Comparison of the catalytic efficiencies shows that D-AB3 is more efficiently  
51 52 incorporated into *E. coli* by 26 folds. The favorable incorporation of D-AB3 into *E. coli* is particularly  
53 54 interesting given the previously reported amino acids that modify peptidoglycans largely favor gram-  
55 56 positive bacteria over gram-negative ones.<sup>28,33,35</sup> The gram-positive selectivity of these amino acids is  
57 58 believed to originate from their poor outer membrane permeability. Indeed, a previously reported  
59 60 fluorescent amino acid D-Lys-FITC in our hands stained *S. aureus* 50 times better than *E. coli*, according  
to our own flow cytometry analysis (Figure S22, SI). A similar magnitude of preference for *S. aureus* was  
reported for a NBD labeled D-Lys by Pires and coworkers.<sup>33</sup>

## Discussion

In this contribution, we describe the fast diazaborine formation of semicarbazide with boronic acid-substituted aryl ketones and aldehydes as exemplified by 2-FPBA, 2-APBA and their derivatives. These conjugation reactions proceed under physiologic conditions with rate constants over  $10^3 \text{ M}^{-1} \text{ s}^{-1}$ , with no need of catalysis. The reaction rate of the diazaborine formation is 2-3 orders of magnitude higher than the widely used azide-alkyne click chemistry.<sup>4</sup> Although phenylhydrazine is known to exhibit similar reactivity, the quick degradation makes it impractical for biological applications. In contrast, semicarbazide shows robust stability in aqueous solution for weeks and possibly months. It is also interesting to compare semicarbazide to acetylhydrazide, which we have previously shown to conjugate with 2-APBA in a quickly reversible manner.<sup>15</sup> The distinct behavior indicates that the acylhydrazone conjugates of 2-APBA and acetylhydrazide are unable to cyclize to give diazaborines, which is presumably due to the weaker nucleophilicity of the  $\alpha$ -nitrogen of acetylhydrazide. With these considerations, semicarbazide appears to reside in the “sweet” spot in reactivity, high enough to afford diazaborines and low enough to avoid degradation. Importantly, the diazaborine formation of semicarbazide encounters little interference from biological media including blood serum and cell lysates except that of the cysteine adduct formation, which affects conjugation with the aldehyde (2-FPBA), not the ketone (2-APBA). Further, semicarbazide is easy to synthesize and derivatize with various labels. These features collectively make the diazaborine formation of semicarbazide an ideal conjugation reaction for biological applications.

To demonstrate the utility of the conjugation chemistry, we show that the diazaborine formation of semicarbazide allows facile labeling of bacterial pathogens. A synthetic amino acid D-AB3, which displays the 2-APBA moiety as its side chain, can be taken up by bacterial cells through the peptidoglycan remodeling mechanism. The cells incorporating D-AB3 can be visualized through conjugation with a fluorophore labeled semicarbazide. A number of synthetic D-amino acids have been shown to covalently modify bacterial peptidoglycans, including several fluorophore-labeled D-lysines or its homologues, as well as D-amino acids with reactive handles. These peptidoglycan modifiers allow fluorescent labeling of various bacteria either directly or through a second conjugation reaction. Toward this end, the use of azide-alkyne click chemistry,<sup>28,30</sup> tetrazine ligation,<sup>36</sup> and alkyne-nitrone cycloaddition<sup>34</sup> have been documented. In comparison, the diazaborine formation is faster than the azide-alkyne click chemistry or the alkyne-nitrone cycloaddition by 2-3 orders of magnitude. Although the tetrazine ligation can be fast, its reaction rate is quite sensitive to how the tetrazine moiety is linked to its biological target<sup>36</sup> and

1  
2  
3 typically bulky diaryl tetrazine derivatives are needed to afford fast kinetics,<sup>37</sup> which are less ideal due to  
4 the outer membrane barrier.  
5  
6

7  
8 Further, it is important to note that our strategy allows for preferential labeling of *E. coli* over several  
9 other bacterial species including *S. aureus*, a gram-positive bacterium. While the bacterial species-  
10 selectivity of the known cell wall modifiers remains to be fully investigated, several amino acids  
11 including D-Lys-FITC are shown to preferentially label gram-positive bacteria over gram-negative strains.  
12 This is perhaps not surprising given the outer membrane barrier of gram-negative bacteria may prevent  
13 the amino acid from accessing peptidoglycan. The fact that D-AB3 is selective for *E. coli* over *S. aureus*  
14 suggests the amino acid can readily pass through the outer membrane of *E. coli*. Importantly, the  
15 elegant work by Kahne and Walker laboratories shows *E. coli* transpeptidase, which is responsible for  
16 peptidoglycan remodeling, prefers aromatic amino acids over aliphatic ones.<sup>38</sup> Given nearly all synthetic  
17 amino acids known to modify peptidoglycans are *aliphatic*, the *aromatic* structure of D-AB3 might be  
18 the underlying reason for its efficient uptake into *E. coli* cells. We submit that investigation of more  
19 structurally diverse cell wall modifiers may enable selective recognition of a variety of bacterial  
20 pathogens.  
21  
22  
23  
24  
25  
26  
27  
28  
29  
30  
31  
32

33 **Supporting Information.** Additional characterization data (NMR, MS and X-ray) of the conjugation  
34 reactions. Detailed protocols and additional microscopic images for bacterial cell labeling.  
35

### 36 **Acknowledgements**

37  
38 We thank Dr. Bo Li for his help on solving the crystal structures of DAB1 and DAB3. We also acknowledge  
39 Dr. Bret Judson and Dr. Patrick Autissier for confocal microscopy and flow cytometry analysis,  
40 respectively. The financial support of this work is provided by the National Institutes of Health through  
41 grant GM102735 to J.G.  
42  
43  
44  
45  
46  
47  
48  
49  
50  
51  
52  
53  
54  
55  
56  
57  
58  
59  
60

## REFERENCES

- 1
- 2
- 3
- 4
- 5 (1) Kolb, H. C.; Finn, M. G.; Sharpless, K. B. *Angew. Chem. Int. Ed.* **2001**, *40*, 2004.
- 6 (2) Prescher, J. A.; Bertozzi, C. R. *Nat. Chem. Biol.* **2005**, *1*, 13.
- 7 (3) Shieh, P.; Bertozzi, C. R. *Org. Biomol. Chem.* **2014**, *12*, 9307.
- 8 (4) McKay, C. S.; Finn, M. G. *Chem. Biol.* **2014**, *21*, 1075.
- 9 (5) Spicer, C. D.; Davis, B. G. *Nat. Commun.* **2014**, *5*:4740.
- 10 (6) Elliott, T. S.; Bianco, A.; Chin, J. W. *Curr. Opin. Chem. Biol.* **2014**, *21*, 154.
- 11 (7) Shih, H.-W.; Kamber, D. N.; Prescher, J. A. *Curr. Opin. Chem. Biol.* **2014**, *21*, 103.
- 12 (8) Kalia, J.; Raines, R. T. *Angew. Chem. Int. Ed.* **2008**, *47*, 7523.
- 13 (9) Dirksen, A.; Dirksen, S.; Hackeng, T. M.; Dawson, P. E. *J. Am. Chem. Soc.* **2006**, *128*, 15602.
- 14 (10) Larsen, D.; Pittelkow, M.; Karmakar, S.; Kool, E. T. *Org. Lett.* **2015**, *17*, 274.
- 15 (11) Dewar, M. J. S.; Dougherty, R. C. *J. Am. Chem. Soc.* **1962**, *84*, 2648.
- 16 (12) Dilek, O.; Lei, Z.; Mukherjee, K.; Bane, S. *Chem. Commun.* **2015**, *51*, 16992.
- 17 (13) Stress, C. J.; Schmidt, P. J.; Gillingham, D. G. *Org. Biomol. Chem.* **2016**, *14*, 5529.
- 18 (14) Bandyopadhyay, A.; Cambray, S.; Gao, J. *Chem. Sci.* **2016**, DOI: 10.1039/C6SC00172F.
- 19 (15) Bandyopadhyay, A.; Gao, J. *J. Am. Chem. Soc.* **2016**, *138*, 2098.
- 20 (16) Kanichar, D.; Roppiyakuda, L.; Kosmowska, E.; Faust, M. A.; Tran, K. P.; Chow, F.; Growziak, M. P.;  
21 Sarina, E. A.; Olmstead, M. M.; Silva, I.; Xu, H. H. *Chem. Biodivers.* **2014**, *11*, 1381.
- 22 (17) Bandyopadhyay, A.; Gao, J. *Chem. Eur. J.* **2015**, *21*, 14748.
- 23 (18) Dirksen, A.; Dawson, P. E. *Bioconjug. Chem.* **2008**, *19*, 2543.
- 24 (19) Blackman, M. L.; Royzen, M.; Fox, J. M. *J. Am. Chem. Soc.* **2008**, *130*, 13518.
- 25 (20) Song, W.; Wang, Y.; Qu, J.; Madden, M. M.; Lin, Q. *Angew. Chem. Int. Ed.* **2008**, *47*, 2832.
- 26 (21) Schmidt, P.; Zhou, L.; Tishinov, K.; Zimmermann, K.; Gillingham, D. *Angew. Chem. Int. Ed.* **2014**, *53*,  
27 10928.
- 28 (22) Tian, M.; Guo, F.; Sun, Y.; Zhang, W.; Miao, F.; Liu, Y.; Song, G.; Ho, C.-L.; Yu, X.; Sun, J. Z.; Wong, W.-Y.  
29 *Org. Biomol. Chem.* **2014**, *12*, 6128.
- 30 (23) Jones, D. P.; Carlson, J. L.; Mody, V. C.; Cai, J.; Lynn, M. J.; Sternberg, P. I. *Free Radic. Biol. Med.* **2000**,  
31 28, 625.
- 32 (24) Strittmatter, N.; Rebec, M.; Jones, E. A.; Golf, O.; Abdolrasouli, A.; Balog, J.; Behrends, V.; Veselkov, K.  
33 A.; Takats, Z. *Anal. Chem.* **2014**, *86*, 6555.
- 34 (25) Lam, H.; Oh, D. C.; Cava, F.; Takacs, C. N.; Clardy, J.; de Pedro, M. A.; Waldor, M. K. *Science*, **2009**,  
35 325, 1552.
- 36 (26) Lupoli, T. J.; Tsukamoto, H.; Doud, E. H.; Wang, T. S.; Walker, S.; Kahne, D. *J. Am. Chem. Soc.* **2011**,  
37 133, 10748.
- 38 (27) Kuru, E.; Hughes, H. V.; Brown, P. J., Hall, E.; Tekkam, S.; Cava, F.; de Pedro M. A.; Brun, Y.  
39 V.; VanNieuwenhze, M. S. *Angew. Chem. Int. Ed.* **2012**, *51*, 12519.
- 40 (28) Liechti, G. W.; Kuru, E.; Hall, E.; Kalinda, A.; Brun, Y. V.; VanNieuwenhze, M.; Maurelli, A. T. *Nature*  
41 **2014**, *506*, 507.
- 42 (29) Siegrist, M. S.; Whiteside, S.; Jewett, J. C.; Aditham, A.; Cava, F.; Bertozzi, C. R. *ACS Chem. Biol.* **2013**,  
43 8, 500.
- 44 (30) Shieh, P.; Siegrist, M. S.; Cullen, A. J.; Bertozzi, C. R. *Proc. Natl. Acad. Sci. U.S.A.* **2014**, *111*, 5456.
- 45
- 46
- 47
- 48
- 49
- 50
- 51
- 52
- 53
- 54
- 55
- 56
- 57
- 58
- 59
- 60

- 1  
2  
3  
4 (31) Fura, J. M.; Sabulski, M. J.; Pires, M. M. *ACS Chem. Biol.* **2014**, *9*, 1480.  
5 (32) Pidgeon, S. E.; Fura, J. M.; Leon, W.; Birabaharan M.; Vezenov, D.; Pires, M. M. *Angew. Chem. Int. Ed.*  
6 **2015**, *54*, 6158.  
7 (33) Sherratt, A. R.; Chigrinova, M.; MacKenzie, D. A.; Rastogi, N. K.; Ouattara, M. T.; Pezacki, A.  
8 T.; Pezacki, J. P. *Bioconjug. Chem.* **2016**, *27*, 1222.  
9 (34) Fura, J. M.; Kearns, D.; Pires, M. M. *J. Biol. Chem.* **2015**, *290*, 30540.  
10 (35) Pidgeon, S. E.; Pires, M. M. *Chem. Commun.* **2015**, *51*, 10330.  
11 (36) Selvaraj, R.; Fox, J. M. *Curr. Opin. Chem. Biol.* **2013**, *17*, 753.  
12 (37) Lebar, M. D.; May, J. M.; Meeske, A. J.; Leiman, S. A.; Lupoli, T. J.; Tsukamoto, H.; Losick, R.; Rudner,  
13 D. Z.; Walker, S.; Kahne, D. *J. Am. Chem. Soc.* **2014**, *136*, 10874.  
14  
15  
16  
17  
18  
19  
20  
21  
22  
23  
24  
25  
26  
27  
28  
29  
30  
31  
32  
33  
34  
35  
36  
37  
38  
39  
40  
41  
42  
43  
44  
45  
46  
47  
48  
49  
50  
51  
52  
53  
54  
55  
56  
57  
58  
59  
60

## TOC Graphic

